Electron spin resonance investigation of the Heavy-Fermion compound CeCu2(Si1−xGex)2

Hans-Albrecht Krug von Nidda, A. Schütz, M. Heil, B. Elschner, Alois Loidl

Angaben zur Veröffentlichung / Publication details:

Krug von Nidda, Hans-Albrecht, A. Schütz, M. Heil, B. Elschner, and Alois Loidl. 1997. "Electron spin resonance investigation of the Heavy-Fermion compound CeCu2(Si1−xGex)2." Applied Magnetic Resonance 12 (2-3): 287–98. https://doi.org/10.1007/bf03162195.

Electron Spin Resonance Investigation of the Heavy-Fermion Compound $CeCu_2(Si_{1-x}Ge_x)_2$

H.-A. Krug von Nidda[1], A. Schütz[1], M. Heil[1], B. Elschner[1], and A. Loidl[2]

[1] Institut für Festkörperphysik, Technische Hochschule Darmstadt, Darmstadt, Germany
[2] Experimentalphysik V, Universität Augsburg, Augsburg, Germany

Abstract. The Kondo-lattice system $CeCu_2(Si_{1-x}Ge_x)_2$ exhibits an alloying induced transition from a coherent Fermi-liquid ($x = 0$) with strongly enhanced effective masses to an antiferromagnetically ordered heavy-fermion system ($x = 1$). This transition is studied by Gd^{3+} ESR in oriented powder samples. The temperature dependence of the ESR line width follows a characteristic pattern which allows one to distinguish between the different ground states. The results obtained in polycrystalline $CeCu_2Si_2$ are in good agreement with the measurements performed in single crystals. Finally we compare our results with ^{63}Cu-NMR data obtained from $CeCu_2Si_2$ and $CeCu_2Ge_2$.

1. Introduction

Heavy fermions are intermetallic compounds containing elements with partially filled 4f or 5f shells (e.g., Ce, Yb, U) on regular lattice sites, also known as Kondo lattices [1]. Their ground state depends on the hybridization strength $J \cdot N(E_F)$ of the local f-moments with the conduction electrons, where J denotes the exchange coupling and $N(E_F)$ is the electronic density of states at the Fermi energy. The decisive mechanism which determines the ground-state properties is the competition between the Kondo screening of the f-moments by the conduction electrons with its characteristic Kondo-lattice temperature $T^* \propto \exp(-1/J \cdot N(E_F))$ and the RKKY-interaction between the f-moments, which is transferred via the conduction electrons with a typical energy scale $T_{RKKY} \propto \exp(-1/J \cdot N(E_F))^2$. The former interaction increases the density of states near E_F. It dominates at large coupling constants J and generates a coherent Fermi liquid of heavy quasiparticles at $T < T^*$. The latter interaction dominates at small J and leads to a magnetically ordered ground state at $T < T_{RKKY}$ [2].

The pseudoternary system $CeCu_2(Si_{1-x}Ge_x)_2$ belongs to the tetragonal $ThCr_2Si_2$ homologs and allows one to tune the competition between the two energy scales as a function of composition [3]. The schematic phase diagram shown in Fig. 1 was

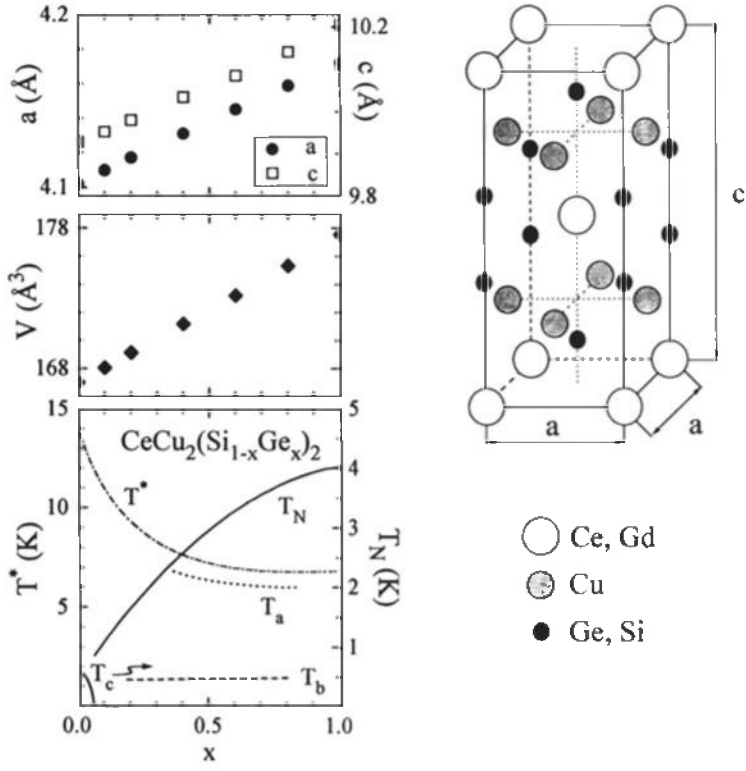

Fig. 1. Crystal structure, lattice parameters a and c, volume V of the unit cell, and phase diagram: Kondo lattice temperature T^*, magnetic phase transitions T_N, T_a, T_b, and superconducting phase T_c.

obtained from susceptibility, resistivity, and specific-heat measurements [4]: $CeCu_2Ge_2$, with a unit-cell volume $V = 177$ Å^3, is an antiferromagnetically ordered heavy-fermion system with $T^* = 6$ K and a Néel temperature $T_N = 4.1$ K. Here Kondo screening and RKKY interaction are of nearly equal strength ($T^* \approx T_{RKKY}$). Replacing germanium by silicon decreases the volume of the unit cell linearly down to $V = 167$ Å^3 for $CeCu_2Si_2$ ($T^* = 15$ K). The decreasing distance between the 4f moments and the ligands increases the hybridization and finally suppresses the magnetic order ($T^* \gg T_{RKKY}$).

The compound $CeCu_2(Si_{1-x}Ge_x)_2$ shows a monotonous decrease of the ordering temperature T_N with decreasing x and develops superconductivity below T_c for $x < 0.08$. A similar behavior is observed by applying hydrostatic pressures. For pressures more than 70 kbar superconductivity is induced in $CeCu_2Si_2$ [5]. Below T_N resistivity and susceptibility measurements yield two further magnetic anomalies at T_a and T_b, which are not fully understood yet.

ESR experiments on single crystals of Gd doped $CeCu_2Si_2$ have been performed some years ago [6]. Gd substitution is necessary, as the $4f^1$ moment of the Ce ion relaxes much too fast to yield any measurable ESR signal. It has been shown that the Gd^{3+} probe (spin $S = 7/2$, angular momentum $L = 0$), which occupies the ce-

rium site, couples to the spin fluctuations of the Ce-4f moments via RKKY interactions yielding a characteristic temperature dependence of the Gd^{3+}-ESR line width. In this report we present our recent Gd^{3+}-ESR results in the whole concentration range $0 \leq x \leq 1$ using oriented powder samples. Gd doped single crystals are hard to grow and were not available. We provide experimental evidence that there is good agreement with the single-crystal measurements in $CeCu_2Si_2$ and we document that Gd^{3+} ESR and ^{63}Cu NMR experiments yield similar results.

2. Model Calculations

2.1. Effect of Crystal Field and Exchange Narrowing on the ESR Signal

The electron spin resonance measures the absorption P_{abs} of the transversal magnetic microwave field as a function of the static magnetic field **H**. The spin-Hamiltonian for the Gd^{3+} probe in a metal with tetragonal crystal symmetry (dominant uniaxial term) is given by [7]:

$$\mathscr{H} = \mu_B \mathbf{H}\,\mathbf{g}\,\mathbf{S} + \frac{1}{3} b_2^0 \left[3S_z^2 - S(S+1)\right] + J_{Gd}\mathbf{S}\boldsymbol{\sigma} \quad . \tag{1}$$

The first term describes the Zeeman interaction of the Gd-spin **S** with the static magnetic field **H** (μ_B: Bohr magneton, **g**: gyromagnetic tensor here is isotropic $g = 2$), which splits the $^8S_{7/2}$-ground state of Gd^{3+} into eight equidistant energy levels $E_m = g\mu_B H m$ $(-7/2 \leq m \leq 7/2)$. The microwave (frequency ν) induces magnetic dipole transitions $\Delta m = \pm 1$ showing a single resonance absorption for $h\nu = g\mu_B H_{res}$, (h denotes the Planck constant).

The second term is caused by the axial crystal-electric field (parameter b_2^0). It shifts the energy levels against each other and therefore causes a fine-structure splitting of the spectrum into seven resonance lines dependent on the polar angle ϑ between the crystallographic c-axis and the magnetic field **H**. For $b_2^0 \ll h\nu$ the energy levels are approximated by

$$E_m = g\mu_B H m + \frac{1}{3} b_2^0 \left[3m^2 - S(S+1)\right] \cdot \frac{1}{2}(3\cos^2\vartheta - 1)$$

yielding the resonance positions

$$g\mu_B H_{m\to m+1} = h\nu - \frac{1}{2} b_2^0 (2m+1)(3\cos^2\vartheta - 1) \quad .$$

The largest crystal-field splitting of the spectrum occurs at $\vartheta = 0°$ with a distance of $2b_2^0$ between neighboring resonances and it vanishes at the magic angle

$\vartheta = 54.7°$. For larger values of b_2^0, one has to diagonalize the sum of Zeeman and crystal-field term and to determine the dipole transitions numerically.

The scattering of the conduction electrons (spin density σ) at the Gd spin by the exchange interaction J_{Gd}, which is described by the third term, leads to a coupling of the seven transitions and causes a narrowing of the ESR spectrum (comparable to the motional narrowing observed in NMR experiments) [8, 9]. In the case of strong exchange narrowing the spectrum again consists of one single resonance line, whereby the crystal field remains visible in the orientation dependence of resonance field H_{res} and line width ΔH: The resonance field is given by the first moment of the seven fine-structure transitions [9]:

$$H_{res} = \sum_m P_m H_{m\to m+1} \quad , \qquad \text{where} \quad P_m = \frac{c_m \exp(-E_m/k_B T)}{\sum_m c_m \exp(-E_m/k_B T)} \quad . \tag{2}$$

For $b_2^0 \ll h\nu$ the transition probability is approximated by $c_m = S(S+1) - m(m+1)$. For $b_2^0 \lesssim h\nu$ the coefficients c_m have to be computed using the exact eigenstates of Zeeman and crystal-field operator. The line width depends on the second moment of all transitions [9]:

$$\Delta H = \Delta H_0 + \Delta H_R + \frac{1}{\delta} \sum P_m (H_{m\to m+1} - H_{res})^2 \quad . \tag{3}$$

ΔH_R is the line width caused by relaxation processes (Section 2.2), ΔH_0 is a constant residual line width originating from impurities and lattice defects, and the factor $1/\delta$ is a function of ΔH_R itself. For a small fine-structure splitting compared with the relaxation $\mu_B \Delta H_R \gg b_2^0$ one obtains $\delta \approx 2\Delta H_R$ [8].

For larger fine-structure splittings, $b_2^0 \lesssim \mu_B \Delta H_R$ the spectrum is only partially exchange narrowed. This means that especially those transitions which are far away from the first moment of all transitions do not take part in the narrowing process. But these outer transitions lead to an overestimation of the second moment in Eq. (3). As the narrowed resonance is of much stronger intensity than those transitions which are not involved in the narrowing process, it is often impossible to decide from the ESR spectra whether it is fully or partially exchange narrowed.

2.2. Relaxation in Heavy Fermions

The ESR line width ΔH_R is proportional to the transversal relaxation rate $1/T_2$ of the Gd spin. The spin-lattice relaxation is determined by the longitudinal relaxation rate $1/T_1$. As in metals both rates are equal ($1/T_1 = 1/T_2$), the relaxation processes are directly obtained from the line width. For intermetallic Ce compounds two relaxation contributions must be taken into account [10]:

$$\Delta H_R = \Delta H_K + \Delta H_{Ce} \quad . \tag{4}$$

The first term ΔH_K is the usual Korringa relaxation caused by the exchange interaction. It is linear in the temperature T [7]:

$$\Delta H_K = \frac{\pi k_B}{g\mu_B} \left\langle J_{Gd}^2(q) \right\rangle N^2(E_F)\, T = bT \quad . \tag{5}$$

$\langle J_{Gd}^2(q) \rangle$ is the exchange integral averaged over the momentum transfer q from the scattering of the conduction electrons at the Gd spin.

The second term ΔH_{Ce} originates from the Ce-4f moments which are fluctuating with a correlation time τ (Fig. 2) according to the fluctuation-dissipation theorem. These spin fluctuations are transferred to the Gd spin via RKKY interactions as an effective fluctuating magnetic field determined by the static Ce susceptibility χ_{Ce}^0 and the RKKY coupling $\lambda_{CeGd}^2(R_i)$ summed up over the Ce moments at a distance R_i [10]:

$$\Delta H_{Ce} = \frac{2k_B}{g_{Ce}^2 g_{Gd} \mu_B^3 \hbar}\, T \chi_{Ce}^0 \tau \sum_i \lambda_{CeGd}^2(R_i) \quad . \tag{6}$$

Assuming a temperature independent $\lambda_{CeGd}^2(R_i)$, Fig. 3 shows the temperature dependence of the line width as expected for ideal heavy-fermion systems: At temperatures $T \ll T^*$, the Ce-4f momentum is completely screened by the conduction electrons; a large Pauli-like susceptibility χ_{Ce}^0 and a large, temperature independent correlation time τ yield a strongly enhanced Korringa like increase in ΔH. At temperatures $T > T^*$, the Ce susceptibility follows a Curie-Weiss law $\chi_{Ce}^0 = (T + \Theta)^{-1}$ with $\Theta = \sqrt{2}\, T^*$ [11] and the correlation time τ decreases according to $1/\tau \propto \sqrt{T}$ [12]; therefore the Ce contribution ΔH_{Ce} decreases with increasing temperature and for $T \gg T^*$ only the usual Korringa contribution ΔH_K remains.

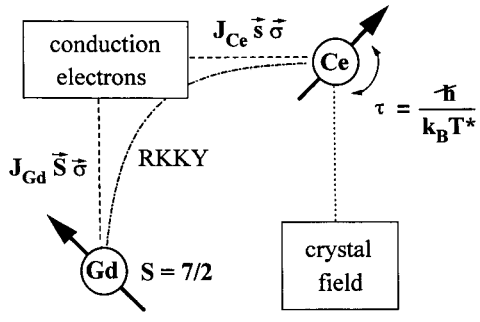

Fig. 2. Schematic representation of the Gd^{3+} relaxation via RKKY interaction to the Ce-4f spin fluctuations.

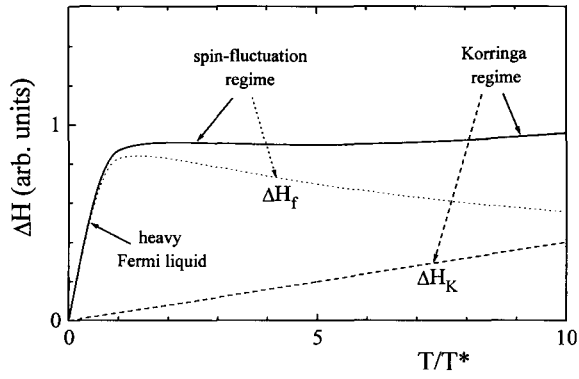

Fig. 3. Model calculation for the ESR-line width ΔH: dashed – Korringa contribution ΔH_K, dotted – Ce-4f contribution ΔH_f.

3. Sample Preparation and Experimental Set-Up

Polycrystalline samples of $Ce_{1-x}Gd_yCu_2(Si_{1-x}Ge_x)_2$ ($y \leq 2\%$) were melted together stoichiometrically from the elements (purity better than 99.99%) in an argon-arc furnace and annealed for two days at 900°C. X-ray diffraction and microprobe analysis proved the proper $ThCr_2Si_2$ structure and did not reveal any parasitic phases. The ESR measurements were performed with a Varian E-101 spectrometer working at $\nu = 9.2$ GHz in the temperature range $1.5 \leq T \leq 300$ K. For cooling a continuous-flow helium-cryostat (Oxford Instruments) was used for $T > 4.2$ K and a cold-finger bath-cryostat below liquid helium temperatures. The magnetic field was controlled by a temperature stabilized hall probe (Bruker). To obtain single-crystal like behavior the polycrystalline samples were powdered to single-crystalline grains of a diameter smaller than 40 μm, immersed in paraffin, and oriented along the crystallographic c-axis within a static magnetic field of 20 kG by liquefying the paraffin.

4. Results

4.1. Orientation Dependence

The observed ESR signal of all samples ($0 \leq x \leq 1$) consists of a broad resonance line. Its resonance field H_{res} (near $g = 2$) and line width ΔH depend on the polar angle ϑ between the crystallographic c-axis and the static magnetic field H. Figure 4 shows typical ESR spectra of $CeCu_2Si_2$ at different angles. They are well fitted by a single resonance line of Dysonian shape [13]:

$$\frac{\mathrm{d}}{\mathrm{d}H} P_{\mathrm{abs}} \sim \frac{\mathrm{d}}{\mathrm{d}H} \frac{\left[\Delta H + \alpha(H - H_{\mathrm{res}})\right]}{(H - H_{\mathrm{res}})^2 + \Delta H^2} \quad . \tag{7}$$

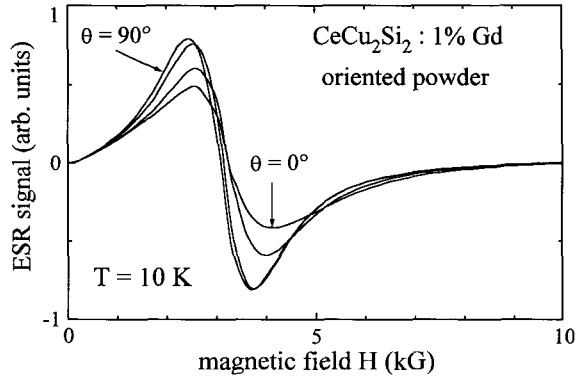

Fig. 4. ESR spectra from oriented powder samples of $CeCu_2Si_2$ doped with 1% Gd for different orientations $\vartheta = \angle(\mathbf{H},\mathbf{c})$.

This is a Lorenzian line which includes both absorption χ''_{Gd} and dispersion χ'_{Gd} ($0 \leq \alpha \leq 1$), because the skin effect drives electric and magnetic microwave components out of phase in metals [14]. The distortion-to-absorption ratio α is used as fit parameter. For samples large compared to the skin depth of the microwave field one finds an asymmetric line shape with $\alpha = 1$, whereas for very small samples α reaches zero, which yields a symmetric resonance line as in dielectrics. Obviously the powder particles of our samples are small compared to the skin depth, because the observed ESR spectra (Fig. 4) are quite symmetric. The angular dependences of resonance position $H_{res}(\vartheta)$ and line width $\Delta H(\vartheta)$ of the oriented powder sample (Fig. 5) are in very good agreement with the data obtained from single crystals [15]. To fit the resonance positions we used Eq. (2), where we determined the transitions numerically from the diagonalized Zeeman and crystal-field operator [16]. The data are well fitted by a crystal-field parameter $b_2^0/h \approx 0.9$ GHz. The value obtained from the single-crystal data is about 5% higher than that obtained from the oriented powder possibly due to an imperfect orientation. For the same reason the line-width data of the powder sample are nearly 100 G larger than those of the single crystal. The simulation of the angular dependence of the line width using the crystal-field parameter b_2^0 obtained from the resonance positions and δ for small fine-structure splitting exhibits deviations around $\vartheta = 90°$ for both the single crystal and the oriented powder samples. The minimum which is expected near $\vartheta = 54.7°$ is only weakly indicated in the experimental data. Here we are obviously at the transition from fully to partially exchange narrowed spectra, where Eq. (3) can only be used as an approximation.

Replacing a few percent of silicon by germanium strongly raises b_2^0. For $x = 0.1$ we estimated $b_2^0/h \approx 1.6$ GHz from the angular dependence of the resonance position. For the other compounds ($x \geq 0.2$) b_2^0 increases further but only weakly from this value. Furthermore the ESR spectra deviate from the Dysonian shape for angles near $\vartheta = 0°$ where the fine-structure splitting reaches its maximum.

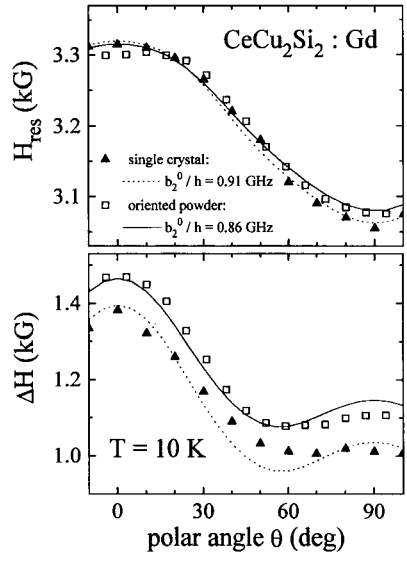

Fig. 5. Resonance field H_{res} (upper picture) and line width ΔH (lower picture) as a function of the polar angle ϑ: Open squares – oriented powder sample doped with 1% Gd at the Ce site, full triangles – single crystal [15] doped with 5% Gd.

This demonstrates that we deal with partially exchange narrowed spectra. For $x > 0$ the line width reaches its minimum at $\vartheta \approx 90°$. We have simulated ESR spectra at X-band frequencies for large b_2^0 ($b_2^0/h \gtrsim 2.0$ GHz) using Eqs. (2) and (3). We found a broad minimum of the line width for $\vartheta \approx 90°$ in accordance with the experiment.

4.2. Temperature Dependence

To keep the influence of the crystal field as small as possible we performed the temperature dependent measurements at the polar angle ϑ, where we observed the minimum of the line width (near 54.7° for $x = 0$ and 90° for all the other compounds).

Figure 6 shows the line width as a function of the temperature for all investigated compounds. For $x = 0$ we observe the typical heavy-fermion behavior described in Section 2.2. Similar results were obtained in single crystalline material [6]. The line width strongly increases for $T \ll T^*$ in the heavy-fermion regime, flattens above T^* in the spin-fluctuation regime, and finally reaches the usual Korringa regime at $T \gg T^*$. With increasing x the decreasing Kondo compensation of the Ce-4f moments gives smaller Curie-Weiss temperatures Θ of χ^0_{Ce}. This increases the line-width contribution ΔH_{Ce}. The compound $x = 0.1$ still behaves like $x = 0$. For $x = 0.2$ the influence of magnetic order becomes visible

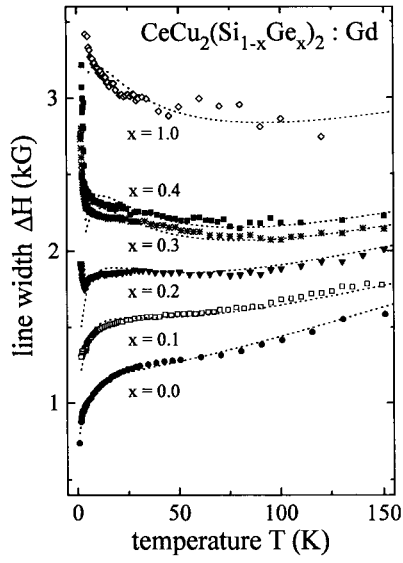

Fig. 6. Line width ΔH as a function of the temperature T for different x at the angle ϑ of minimum line width (54.7° for $x = 0$, 90° for the other compounds). The dotted lines are fit curves to the data above the ordering temperature T_N according to Eq. (8). Below T_N the magnetic order leads to an inhomogeneous line broadening. T^* is taken from the phase diagram (Fig. 1), $b \approx 4$–5 G/K, $\Delta H_0(x = 0.0$–$1.0) = 600$–1600 G, $C(x = 0.0$–$1.0) = 4.4$–9.3.

as a weak line broadening at lower temperatures around the ordering temperature T_N. The line broadening below T_N becomes much stronger in the compounds $x \geq 0.3$ and at T_a the line finally disappears. This inhomogeneous line broadening below the ordering temperature is caused by internal fields from the incommensurate magnetic order of the Ce spins. For $x = 1$ the influence of the susceptibility clearly dominates the temperature dependence of the line width. Below T_N the line disappears rapidly. The line-width data were fitted using Eq. (4) in the following form:

$$\Delta H = \Delta H_0 + bT + CT \frac{1}{T + \sqrt{2} \cdot T^*} \cdot \frac{1}{\sqrt{T}} \quad . \tag{8}$$

For all compounds under consideration we assume an inverse square-root law for the temperature dependence of the spin-correlation time τ [12]. This is confirmed by inelastic neutron scattering for the compounds $x = 0$ [17] and $x = 1$ [18]. There the line width $\Gamma(T) \propto 1/\tau$ of the quasielastic peak approximately followed a square-root law: $\Gamma \approx 0.4 \text{ meV} \cdot \sqrt{T/K}$ for $x = 0$ and $\Gamma \approx 0.12 \text{ meV} \cdot \sqrt{T/K}$ for $x = 1$. The characteristic temperature T^* which determines the susceptibility χ^0_{Ce} is taken from the phase diagram. The Korringa contribution is about $b \approx 4-5$ G/K for all samples. To simplify the evaluation we avoid any further crystal-field corrections apart from a constant residual line-width contribution ΔH_0, which in-

creases with x from 0.6 kG for $x = 0$ to 1.6 kG for $x = 1$, due to the increase of the crystal-field parameter b_2^0. The fits of the model function, Eq. (8), provide a rough agreement with the experimental results. The fact that Γ is about three times smaller for $x = 1$ [18], compared to $x = 0$ [17], yields an increase of C by a factor of 3. This increase in C is documented by the increase in ΔH (Fig. 6) due to much stronger contributions from spin fluctuations.

5. Discussion

To confirm our Gd^{3+}-ESR results we compare them to ^{63}Cu-NMR experiments, which directly measure the nuclear spin-lattice relaxation rate $(1/T_1)_{NMR}$. Similar to ΔH_{ESR} in Eq. (4) the nuclear relaxation $(1/T_1)_{NMR}$ consists of the purely metallic Korringa relaxation and an additional contribution of the Ce-4f moments where the electronic exchange coupling has to be replaced by the hyperfine coupling of the nuclear copper spin to the electronic system. Figure 7 shows the NMR-relaxation rate of $CeCu_2Ge_2$ [19, 20] and $CeCu_2Si_2$ [21] together with the Gd^{3+}-line width after subtraction of the residual line width obtained from our fit function. For $CeCu_2Ge_2$ we observe a comparable behavior of ESR-line width and NMR-relaxation rate above the ordering temperature T_N. Below T_N the comparison is impossible as the ESR-signal vanishes due to the strong inhomogeneous broadening. It should be mentioned that the NMR line shows a broadening from inhomogeneous internal fields below T_N as well [20]. The data of $CeCu_2Si_2$ co-

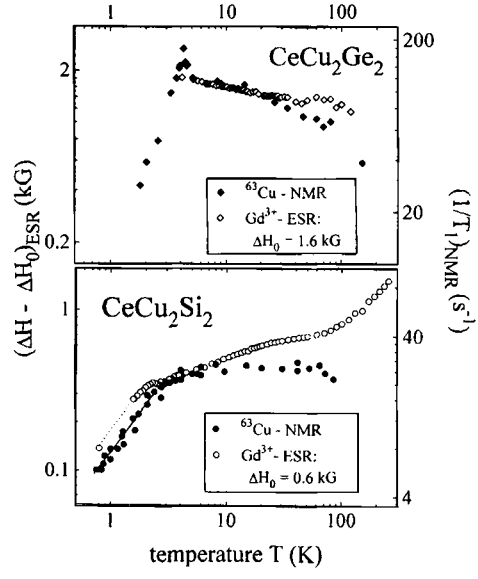

Fig. 7. Temperature dependence of the Gd^{3+}-line width ΔH for $x = 0$ and $x = 1$ compared to the ^{63}Cu-NMR spin-lattice relaxation rate $1/T_1$ [19, 20]. The line width at $T = 0.8$ K was measured in a liquid ^3He bath cryostat.

incide very well especially at lowest temperatures where the heavy-fermi liquid is realized. At higher temperatures where the transition to the normal metallic Korringa behavior occurs, clear deviations between the ESR line width and the nuclear spin-lattice relaxation rate become apparent. To understand this discrepancy one has to compare the relation of the low-temperature increase of both ΔH_{ESR} and $(1/T_1)_{NMR}$ with their typical metallic Korringa contribution. This can be done using the reference systems $LaCu_2Ge_2$ or $LaCu_2Si_2$. The Gd^{3+} ESR in $LaCu_2Si_2$ [6] obeys a Korringa law which coincides very well with the high temperature dependence of $b = 5$ G/K observed in $CeCu_2Ge_2$. For $LaCu_2Ge_2$ a nuclear ^{63}Cu Korringa rate $1/(T_1T) = 0.073/(sK)$ has been published [19] which is comparable to 0.097/(sK) in $LaCu_{2.2}Si_2$ (Büttgen N., private communication). Below 2 K the ESR line width reveals a Korringa slope of approximately 150 G/K, which is an enhancement of 30 compared to the high temperature Korringa slope. At low temperatures the NMR-relaxation rate increases by 8/(sK) revealing an enhancement by a factor of 100. This fact proves the local character of the Ce-4f hybridization and the relaxation mechanism via RKKY interaction: If the hybridization were spread over the whole conduction band, normal Korringa and 4f contribution should exhibit the same relative strength for both the ESR and the NMR probe. But the RKKY interaction strongly depends on the distance between the 4f moments and the respective probe. The corresponding squared matrix elements, which determine the relaxation rate, decrease proportional $1/R^6$ with increasing distance R of the probe to the Ce-4f momentum [22]. As one can see from the crystal structure the next Cu neighbor of the Ce ion (R_{min}(Cu-Ce) = $= \sqrt{(a/2)^2 + (c/4)^2}$) is only about 3/4 of distance of the Ce-Ce(Gd) separation (R_{min}(Gd-Ce) = a). This simple estimation yields a relative strength of the 4f contribution compared to the usual Korringa relaxation which is 5 times higher for the ^{63}Cu NMR than for the Gd^{3+} ESR. This estimate agrees well with the experimental result where the 4f-contribution is more than 3 times larger for NMR than for ESR.

6. Conclusion

We have investigated the pseudoternary Kondo-lattice system $CeCu_2(Si_{1-x}Ge_x)_2$ by Gd^{3+} ESR. We have shown that the orientation of powder samples is a successful method to obtain information comparable to single-crystal data. With increasing x the transition from the heavy-fermion ground state to magnetic order is nicely probed by the Gd^{3+}-line width. Its temperature dependence above the ordering temperature T_N is well described by the Ce-4f spin fluctuations which are transferred to the Gd^{3+} spin via RKKY interaction. The inhomogeneous line broadening below T_N is due to internal fields connected with the incommensurate magnetic order of the Ce-4f moments. The comparison with the ^{63}Cu-NMR relaxation rate confirms the local character of the Ce-4f hybridization and the validity of the RKKY mechanism which strongly depends on the distance between the Ce and the NMR or ESR probe.

Acknowledgements

We are grateful to F. Fischer for the preparation of the samples. This work was supported by the Deutsche Forschungsgemeinschaft within Sonderforschungsbereich 252.

References

[1] Grewe N., Steglich F.: Handbook on the Physics and Chemistry of Rare Earths, vol. 14. Amsterdam: Elsevier Science B.V. 1991.
[2] Doniach S.: Physica B **91**, 231 (1977)
[3] Trovarelli O., Weiden M., Müller-Reisner R., Gómez-Berisso M., Sereni J.G., Geibel C., Steglich F.: Physica B **223-224**, 295 (1995)
[4] Knebel G., Eggert C., Engelmann D., Viana R., Krimmel A., Dressel M., Loidl A.: Phys. Rev. B **53**, 11586 (1996)
[5] Jaccard D., Behnia K., Sierro J.: Phys. Lett. A **163**, 475 (1992)
[6] Schlott M., Elschner B., Herrmann M., Assmus W.: Z. Physik B: Condens. Matter **72**, 385 1988
[7] Barnes S.E.: Adv. Phys. **30**, 801 (1981)
[8] Barnes S.E.: Phys. Rev. B **9**, 4789 (1974)
[9] Plefka T.: phys. stat. sol. (b) **55**, 129 (1973)
[10] Coldea M., Schäffer H., Weissenberger V., Elschner B.: Z. Physik B: Condens. Matter **68**, 25 (1987)
[11] Callaway J.: Quantum Theory of the Solid State, p. 448. New York: Academic Press 1991.
[12] Cox D.L., Bickers N.E., Wilkins J.W.: J. Appl. Phys. **57**, 3166 (1985)
[13] Feher G., Kip A.F.: Phys. Rev. **98**, 337 (1955)
[14] Dyson F.J.: Phys. Rev. **98**, 349 (1955)
[15] Schlott M.: Ph.D. Thesis 1989.
[16] Spitzfaden R.: Ph.D. Thesis 1996.
[17] Horn S., Holland-Moritz E., Löwenhaupt M., Steglich F., Scheuer H., Benoit A., Flouquet J.: Physica B **107**, 103 (1981)
[18] Loidl A., Krimmel A., Knorr K., Sparn G., Lang M., Geibel C., Horn S., Grauel A., Steglich F., Welslau B., Grewe N., Nakotte H., de Boer F.R., Murani A.P.: Ann. Physik (Germany) **1**, 78 (1992)
[19] Büttgen N., Böhmer R., Loidl A.: Solid State Commun. **93**, 753 (1995)
[20] Büttgen N., Böhmer R., Krimmel A., Loidl A.: Phys. Rev. B **53**, 5557 (1996)
[21] Asayama K., Kitaoka Y., Kohori Y.: JMMM **76-77**, 449 (1988)
[22] Cox D.L.: Phys. Rev. B **35**, 6504 (1987)

Author's address: Dr. Hans-Albrecht Krug von Nidda, Institut für Festkörperphysik, TH Darmstadt, Hochschulstraße 6, D-64289 Darmstadt, Germany